2D MHD MODELS OF THE LARGE SCALE SOLAR CORONA

Eirik Endeve*†, Thomas E. Holzer† and Egil Leer*†

*Institute of Theoretical Astrophysics, P.O. Box 1029 Blindern, N-0315 Oslo Norway
†High Altitude Observatory, NCAR, P.O. Box 3000, Boulder Colorado 80307 USA

Abstract. By solving the equations of ideal MHD the interaction of an isothermal coronal plasma with a dipole-like magnetic field is studied. We vary the coronal temperature and the magnetic field strength to investigate how the plasma and the magnetic field interact to determine the structure of the large scale solar corona. When our numerical calculations are initiated with an isothermal solar wind in a dipole magnetic field, the equations may be integrated to a steady state. Open and closed regions are formed. In the open regions the atmosphere expands into a super-sonic wind, and in the closed regions the plasma is in hydrostatic equilibrium. We find that the magnetic field configuration in the outer corona is largely determined by the equatorial current sheet.

INTRODUCTION

Observations from the Ulysses space craft indicate that the solar wind exhibits large variations with heliographic latitude [1]. At solar minimum the solar magnetic field is close to that of a tilted dipole. Fast wind emanates from higher latitudes, whereas the slow wind is observed at lower latitudes. This variation is believed to be closely related to the interaction between the solar wind and the coronal magnetic field. The inertial, gravitational and pressure gradient forces in the stratified solar atmosphere together with magnetic forces determine the large scale structure of the solar corona.

In order to study the force balance in an axially symmetric magnetized solar corona, and the coupling between the outflowing plasma and the coronal magnetic field, we use the equations of ideal MHD to model an isothermal flow from the base of the corona ($r = 1R_s$) to 15 solar radii. Here R_s is the radius of the Sun.

This is essentially the problem solved by Parker in 1958 [2], but here we have included a solar dipole field, and the problem is solved self consistently in a MHD formulation. Problems of this type were first addressed by Pneuman and Kopp in 1971 [3]. Since the paper by Pneuman and Kopp 1971 many have worked on problems on gas-magnetic field interactions in the solar wind: See Bravo and Stewart 1997 [4] and the references therein.

EQUATIONS

To study the interaction between the ionised plasma of the outer solar atmosphere and the coronal magnetic field we apply the time dependent equations of ideal MHD:
Continuity equation:

$$\frac{\partial \rho}{\partial t} + \nabla \cdot (\rho \mathbf{u}) = 0 \tag{1}$$

Momentum equation:

$$\frac{\partial (\rho \mathbf{u})}{\partial t} + \nabla \cdot (\rho \mathbf{u}\mathbf{u}) = -\nabla P - \frac{GM_s}{r^2}\rho \mathbf{e}_r + \mathbf{J} \times \mathbf{B} \tag{2}$$

Ampère's law:

$$\mathbf{J} = \frac{1}{\mu_0}\nabla \times \mathbf{B} \tag{3}$$

Ohm's law:

$$\mathbf{E} = -(\mathbf{u} \times \mathbf{B}) \tag{4}$$

Induction equation:

$$\frac{\partial \mathbf{B}}{\partial t} = -\nabla \times \mathbf{E} \tag{5}$$

Here $\rho\ (= m_p n), \mathbf{u}, P, \mathbf{J}, \mathbf{B}$ and $\mathbf{E}$ are mass density, flow velocity, gas pressure, electric current density, magnetic field and electric field, respectively. G, M_s, m_p and μ_0 are the gravitational constant, the solar mass, the proton mass and the magnetic permeability. The gas pressure is given by the ideal gas law, $P = 2nkT$.

In order to study the acceleration of high- and low-speed solar wind one must include a realistic energy

CP679, *Solar Wind Ten: Proceedings of the Tenth International Solar Wind Conference,*
edited by M. Velli, R. Bruno, and F. Malara

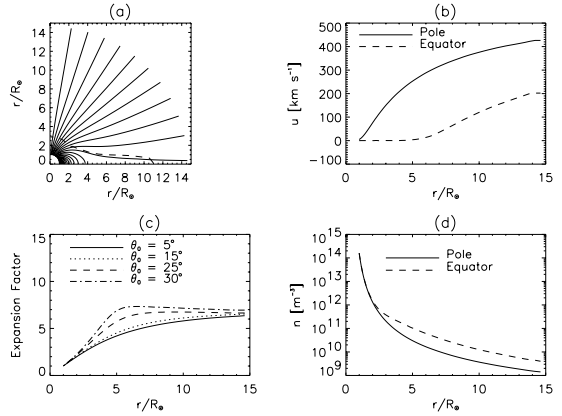

FIGURE 1. Solution to the MHD equations for a temperature $T = 1.25 \times 10^6$ K, and a coronal base pressure $P_0 = 5.5 \times 10^{-3}$ N m^{-2}. At the coronal base the magnetic field strength is $B_0 = 7 \times 10^{-4}$ T at the pole. Panel (a): Magnetic field configuration. The dashed line is where the flow becomes super-sonic. Panel (b): Radial flow velocity versus heliocentric distance at the pole (Solid line) and the equator (dashed line). Panel (c): Expansion factor, f_{exp}, versus heliocentric distance for selected field lines emanating from the solar surface at a colatitude θ_0. Panel (d): Electron density versus radial distance for the pole (solid line) and the equator (dashed line).

equation including an appropriate heating mechanism. However, this is not the focus of the present paper. We are interested in studying the force balance in the system. In order to make the problem as simple as possible we take the temperature to be a constant throughout the solar atmosphere.

RESULTS

The equations are solved in spherical coordinates (r, θ, ϕ), assuming axial symmetry. We have discretized the equations on a 129×65 nonuniform (r, θ) grid, where our computational domain extends from $r = 1R_s$ to $15R_s$ in r, and from 0 to π in θ. We use a MHD code developed by Nordlund and Galsgaard 1995 (only available on the web http://www.astro.ku.dk/∼kg) modified to handle spherical coordinates. Our boundary conditions at the coronal base, $r = 1R_s$, are uniform in θ. At the outer boundary the flow is super-sonic. There we use simple extrapolations to calculate our boundary conditions.

Figure 1 is a plot of a solution to Eqs. (1)-(5) initiated with a dipole field and a spherically symmetric isothermal solar wind with a temperature of 1.25×10^6 K and a base pressure of $P_0 = 5.5 \times 10^{-3}$ N m^{-2}. The magnetic field strength at the coronal base is $B_0 = 7 \times 10^{-4}$ T at the pole. The solar wind causes the dipole to open and form flow tubes down to a colatitude of about 30 degrees. In the closed regions the atmosphere is in hydrostatic equilibrium. In this model the closed region extends out to about 5 solar radii at the equator. In the open regions a field aligned wind is allowed to expand into interplanetary space. The open regions and the hydrostatic closed regions, frequently referred to as a helmet streamer, are separated by a thin current sheet. Above the helmet streamer, in the equatorial plane, there is a current sheet separating the northern and southern hemispheres where the magnetic field has opposite polarity. This equatorial current sheet determines the structure of the large scale magnetic field, and the geometry of the individual flow tubes.

A flow tube with a cross section A_0 at the coronal base expands with heliocentric distance to a cross section $A(r)$ at a radial distance r. To study the expansion of an individual flow tube we define the expansion factor [5]:

$$f_{exp}(r) = (\frac{B_0}{B(r)})(\frac{R_s}{r})^2, \qquad (6)$$

where B_0 is the magnetic field strength in the flow tube at the coronal base, and $B(r)$ is the field strength in the flow tube at a radial distance r.

In Figure 1 (c) we plot the expansion factor versus radial distance for flow tubes emanating at a colatitude θ_0 at the solar surface. Notice that the individual flow tubes expand super-radially in the inner corona approaching a constant value of about 7 at the outer boundary. Beyond the outer boundary the magnetic field falls off as r^{-2}. At the outer boundary there is a difference of more than 200 km s^{-1} in the radial flow speed from the equator to the pole (see Figure 1 b). At the equator the flow is sub sonic inside $r = 11R_s$, whereas the flow becomes super-sonic at about 3 solar radii in the polar region. In panel (d) we see that the density scale height is larger at the equator than near the pole. The high pressure in the equator region is localized in θ; it extends over some five degrees. This high pressure in the equator produces an axial current. The $\mathbf{J} \times \mathbf{B}$ force balances the pressure gradient force.

Varying coronal temperature

In Figure 2 and Figure 3 we plot characteristics of the solutions to the MHD equations where the coronal temperature has been varied from 1.0×10^6 K to 2.0×10^6 K. The electron density at the inner boundary is adjusted in order to fix the coronal base pressure to $P_0 = 5.5 \times 10^{-3}$ N m^{-2}. The magnetic field strength at the coronal base is 7×10^{-4} T at the pole. This corresponds to a plasma β ($= \frac{P}{B^2/2\mu_0}$) of about 3×10^{-2}.

The increase in temperature causes the proton flux density at 1 AU to increase from 4.6×10^{11} (5.7×10^{11})

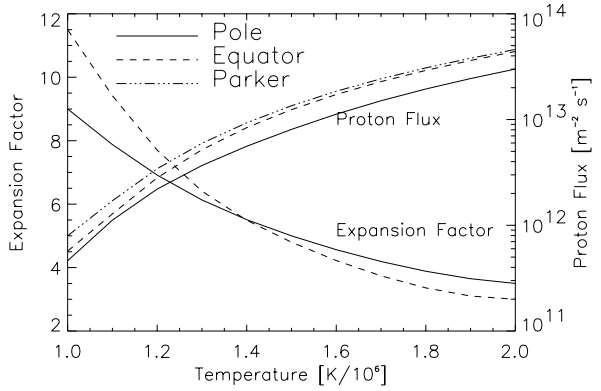

FIGURE 2. Solutions to the MHD equations where the temperature in the corona is varied from 1×10^6 K to 2×10^6 K. The electron density at the inner boundary is adjusted in order to fix the coronal base pressure to $P_0 = 5.5 \times 10^{-3}$ N m^{-2}. The magnetic field strength at the coronal base is $B_0 = 7 \times 10^{-4}$ T. The ascending lines are plots of the proton flux, scaled to 1 AU, for the polar (solid line) and equatorial (dashed line) regions. We also plot the proton flux for a spherically symmetric isothermal flow (dash-dot-dot-dot line). The descending lines are plots of the expansion factor at the outer boundary, $r = 15R_s$, for field lines emanating from latitudes near the pole (solid line) and for open field lines emanating from latitudes near the closed field regions (dashed line).

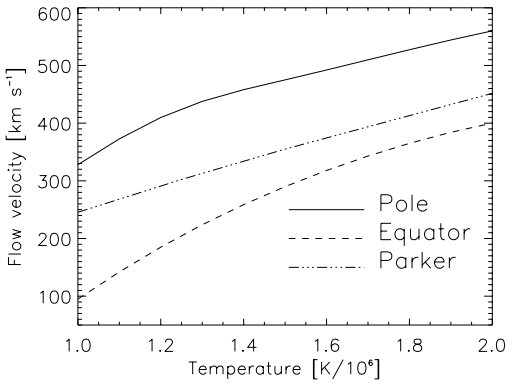

FIGURE 3. Same solutions as in Figure 2, but here we plot the radial flow velocity at the outer boundary, $u_r(15R_s)$, versus coronal temperature for the polar (solid line) and the equatorial (dashed line) regions. We also plot the flow speed at $r = 15R_s$ for a spherically symmetric isothermal Parker wind (dash-dot-dot-dot).

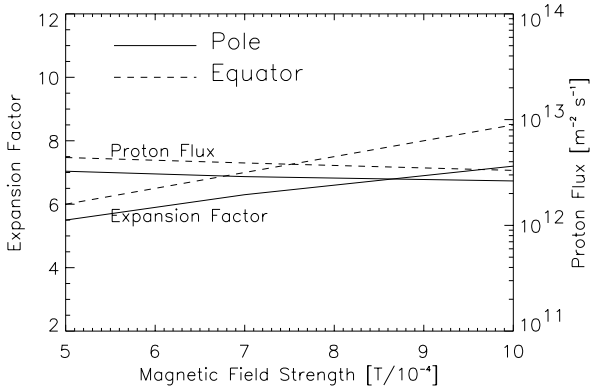

FIGURE 4. Solutions to the MHD equations where the magnetic field strength at the inner boundary is varied. The field strength at the pole, B_0, is varied from 5×10^{-4} T to 1×10^{-3} T. The coronal temperature is 1.25×10^6 K, and the coronal base pressure is $P_0 = 5.5 \times 10^{-3}$ N m^{-2}. The plot is similar to Figure 2. Ascending lines are the expansion factor at 15 solar radii. Descending lines are the proton flux scaled to 1 AU.

m^{-2} s^{-1} to 3.0×10^{13} (4.4×10^{13}) m^{-2} s^{-1} for the polar (equatorial) regions. For a more massive wind the magnetic flux at the outer boundary increases. The expansion factor at $15R_s$ decreases from 9 (11.5) to 4.0 (3.5). The increase in magnetic flux in the wind is consistent with an increased current in the equatorial region. The integrated current in the equatorial sheet increases by more than a factor five when the temperature is increased by a factor two. The flow velocity at the outer boundary increases from 328 (90) km s^{-1} to 560 (400) km s^{-1}. For comparison we also plot solutions for a spherically symmetric isothermal corona. The dash-dot-dot-dot lines (termed Parker in Figures 2 and 3) are solutions to the exact same problem where the magnetic field is set to zero (or is purely radial). Notice that the super-radial expansion of flow tubes at high latitudes (produced by the equatorial current sheet) leads to a faster wind than what was found by Parker [6].

Varying magnetic field strength

In Figures 4 and 5 we plot results for models where the magnetic field strength at the coronal base has been varied from 5×10^{-4} T to 1×10^{-3} T at the pole. The temperature is set to 1.25×10^6 K, and the coronal base pressure is fixed to $P_0 = 5.5 \times 10^{-3}$ N m^{-2}. This corresponds to a plasma β changing from 1.4×10^{-2} to 5.5×10^{-2}.

For an increasing magnetic field strength the proton flux at the orbit of Earth decreases from 3.3×10^{12} (4.4×10^{12}) m^{-2} s^{-1} to 2.6×10^{12} (3.3×10^{12}) m^{-2} s^{-1} for the polar (equatorial) regions. The expansion factor at the outer boundary, $r = 15R_s$, increases from 5.5 (6.0) to 7.2 (8.5). The flow velocity at the outer boundary increases from 405 km s^{-1} to 450 km s^{-1} in the polar region, whereas at the equator it decreases from 240 km s^{-1} to

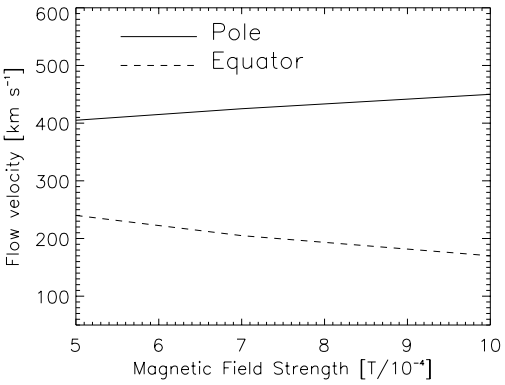

FIGURE 5. Same solutions as in Figure 4. Here we plot the radial flow velocity at the outer boundary, $r = 15R_s$, for the pole (solid line) and the equator (dashed line), versus magnetic field strength at the coronal base.

170 km s^{-1}. Notice that a non-magnetic, isothermal solar wind, with $T = 1.25 \times 10^6$ K and $P_0 = 5.5 \times 10^{-3}$ N m^{-2} yields a proton flux at 1 AU of $(nu)_E = 4.6 \times 10^{12}$ m^{-2} s^{-1}, and a flow speed at $r = 15R_s$ of 303 km s^{-1} (see Figures 2 and 3).

For a stronger magnetic field at the coronal base the magnetic forces in the inner corona becomes more dominant. For $B_0 = 5.0 \times 10^{-4}$ T the atmosphere is in hydrostatic equilibrium out to $4R_s$ at the equator, while for $B_0 = 1.0 \times 10^{-3}$ T the closed field region extends out to $6R_s$ at the equator. A stronger magnetic field does not produce the significant changes in the corona as the change in temperature. The proton flux at 1AU, the expansion factor and the flow speed at the outer boundary change by less than 50 percent. The current sheet in the equatorial region stays relatively unchanged. When the magnetic field strength in the inner corona increases the closed field region extends to a higher latitude. The magnetic flux at the outer boundary relative to the flux at the coronal base decreases. This causes the expansion factor at $r = 15R_s$ to increase. The change in proton flux is determined by two competing factors. For a stronger field the critical point moves inward causing an increase in proton flux, but the super-radial expansion beyond the critical point leads to a decrease in the flux. In our models the latter effect seems to dominate.

DISCUSSION

Our numerical experiments show that for an isothermal solar coronal we are able to construct steady state solutions to Eqs. (1)-(5). The solutions show the same exponential dependence of proton flux with temperature as in spherically symmetric models where the magnetic field is purely radial [7]. We also find that the expansion factor of individual flow tubes decreases rapidly with increasing temperature. This is not the case when we vary the magnetic field strength at the base of the corona.

The isothermal models are able to maintain a fairly high pressure in the equatorial current sheet whereas at higher latitudes, where the flow becomes super-sonic close to the Sun, the pressure falls off more rapidly with heliocentric distance. This results in a pressure gradient force away from equator which is balanced by magnetic forces. Our models demonstrate that an increasing density and temperature in the corona produces a larger solar wind mass flux, a higher pressure in the equator, a larger magnetic flux in the outer corona, and a stronger equatorial current sheet.

In more realistic models, where the temperature is allowed to decrease with heliocentric distance, the equatorial pressure may fall off more rapidly and steady state solutions may not even exists yielding a strongly time dependent reconnection process at equatorial latitudes.

ACKNOWLEDGMENTS

This work was supported by the Norwegian Research Council (NFR) under contract 145519/432. Eirik Endeve thanks the High Altitude Observatory for their hospitality during his visit.

REFERENCES

1. McComas, D. J., Phillips, J. L., Bame, S. J., Gosling, J. T., Goldstein, B. E., and Neugebauer, M., *Space Sci. Rev.*, **72**, 93–98 (1995).
2. Parker, E. N., *Astrophys. J.*, **128**, 664–676 (1958).
3. Pneuman, G. W., and Kopp, R. A., *Sol. Phys.*, **18**, 258–270 (1971).
4. Bravo, S., and Stewart, G., *Astrophys. J.*, **489**, 992–999 (1997).
5. Kopp, R. A., and Holzer, T. E., *Sol. Phys.*, **49**, 43–56 (1976).
6. Holzer, T. E., *J. Geophys. Res.*, **82**, 23–35 (1977).
7. Holzer, T. E., and Leer, E., *J. Geophys. Res.*, **85**, 4665–4679 (1980).